ELSEVIER

Journal of Alloys and Compounds 328 (2001) 8–13

Journal of ALLOYS AND COMPOUNDS

www.elsevier.com/locate/jallcom

Invited lecture

Synchrotron spectromicroscopy in medicine and biology

B. Gilbert[a,*], G. Margaritondo[a], D. Mercanti[b], P. Casalbore[b], G. De Stasio[c]

[a]*Institut de Physique Appliquée, Ecole Polytechnique Fédérale de Lausanne, PH-Ecublens, CH-1015 Lausanne, Switzerland*

[b]*Istituto di Neurobiologia del CNR, Viale Marx 15, 00100 Roma, Italy*

[c]*Department of Physics, University of Wisconsin-Madison and Synchrotron Radiation Center, 3731 Schneider Drive, Stoughton, WI 53589, USA*

Received 13 June 2000; received in revised form 17 June 2000; accepted 22 December 2000

Abstract

The ability to couple high-resolution specimen imaging with chemical state analysis allows problems in biology and medicine to be approached in a novel and powerful way. Element specific chemical state analysis can be performed at tunable synchrotron X-ray sources through core level absorption spectroscopy, and a number of methods have been developed to routinely use this technique at the microscopic scale relevant to cellular phenomena. A diverse range of biological specimens has been studied in the MEPHISTO spectromicroscope, and some results are discussed here. The examples are used to illustrate the ability of spectromicroscopy to obtain certain specific results, such as semi-quantitative element detection, and chemical state elucidation or mapping. Essential practical considerations are also emphasized, including sample preparation, the sensitivity of absorption spectroscopy, interferences between elements, and the use of complementary sample analyses.

Keywords: X-ray imaging; X-ray absorption; Synchrotron spectromicroscopy; MEPHISTO spectromicroscope; Microchemical analysis

1. Introduction

The key characteristic of X-ray radiation emitted from synchrotron sources is high brightness, which has placed X-ray diffraction techniques at the center of structural investigations of macromolecules [1]. In addition, the high spatial coherence of the synchrotron beam enables medical radiology with phase contrast for a higher resolution than conventional sources [2]. The tuneability of the source means the structures of non crystalline materials can be studied through X-ray absorption, as in the EXAFS spectroscopy of metalloproteins [3]. For imaging, X-ray microscopes have a better theoretical resolution limit than optical wavelength equivalents, and are more penetrating and less damaging than electron microscopes [4]. The subject of this contribution is the combination of X-ray microscopy with soft X-ray absorption spectroscopy (henceforth called spectromicroscopy), using the ability to scan the X-ray energy, so that an elemental and chemical analysis may be performed on microscopic areas. Thus, using specific photon energies, the signal from an individual chemical species can be isolated and mapped. A number of spectromicroscopes have been constructed and applied to a wide range of organic specimens [5–7]. The MEPHISTO spectromicroscope was used for the experiments discussed here [8], and operates in a real-time imaging, total electron yield mode with an optimum lateral resolution of 20 nm [9].

The relevance of this technique to the biological sciences stems from the combination of ultra-structural imaging with chemical state analysis, especially for the physiological, low Z elements, which are hard to access with electron microprobe techniques. Much anticipation surrounds efforts to image and perform microspectroscopy on living cells, using sufficiently penetrating X-rays, but the major challenge here is to limit radiation damage. A dose of 10 Gy is typically considered lethal, but may be delivered in milliseconds by third generation synchrotrons and beamlines. The dose constraints are less restrictive for dry, fixed or frozen specimens, and biological specimens are stable enough to allow submicron differentiation of carbon species in DNA or protein [10], and quantitative calcium mapping in bone [11]. An expanding area is the environmental analysis of biofilms, water or rocks, where spectromicroscopy offers the possibility of probing organism-environment redox reactions [12]. Recent trials have shown that spectromicroscopy of minerals and or-

*Corresponding author. Tel.: +1-608-877-2000; fax: +1-608-877-2001.

E-mail address: bgilbert@dpmail.epfl.ch (B. Gilbert).

0925-8388/01/$ – see front matter
PII: S0925-8388(01)01323-8

ganic material at the surface of rock may be performed with little specimen preparation.

The role of spectromicroscopy in medicine (to date, exclusively basic medical research) is less developed. Two active areas of research are within significant medical fields. Firstly, spectromicroscopy [13], along with IR microscopy [14] and nascent magnetic resonance (MR) microscopies [15] have begun to study the complex issues of neurodegenerative diseases such as Alzheimer's. All three techniques are attempting to understand the location and composition of the characteristic denatured protein bundles that form in dementia. In a second example, the microdistribution of drugs relevant to a novel therapy for malignant brain tumor is uncovered by spectromicroscopy of human brain tumor tissues [16,17]. Neutron capture therapy (NCT) aims to target a brain tumor with an isotope (boron-10, or potentially gadolinium-157) possessing a far higher capture cross section for thermal neutrons than other elements present in tissue [18,19]. If the NCT agent is localized only in the tumor, and more specifically, in the nuclei of tumor cells, macroscopic irradiation of the skull with thermal neutrons will result in a localized radiotoxic effect that kills tumor cells, but spares normal tissue.

We have studied the distribution and chemistry of boron and gadolinium based NCT agents in cultures of glioblastoma cells, and in sections of tumor tissues taken from human patients administered an NCT drug prior to surgery for tumor resectioning. Successful experiments of this nature must be able to firstly, detect trace elements in organic matrices at high spatial resolution and secondly, correlate this information to local cell or tissue histology. We discuss these issues, additionally highlighting the need for complementary specimen analyses, and show exemplary results.

2. Materials and methods

A schematic view of the MEPHISTO spectromicroscope installed on a synchrotron ring is given in Fig. 1. The total yield of electrons emitted from the surface under X-ray illumination is proportional to the X-ray absorption coefficient, and hence an X-ray absorption spectrum is acquired by recording the emitted electron intensity from microscopic areas of the sample as a function of the photon energy. A magnified photoelectron image of the specimen is formed by the electron optics of the spectromicroscope and projected onto a detector, converted into an optical image at a phosphor screen, captured by a video camera linked to a PC and digitized. Cells analyzed in MEPHISTO are fixed and dehydrated, and may be analyzed with no further treatment [20], or ashed in a UV/ozone environment [21] to remove carbon with no displacement of the remaining elements detected at >100 nm resolution [22]. This process additionally thins the specimen, aiding analysis which is impossible on thick (>1 μm), insulating samples. Tissue samples for trace element detection are fixed in a paraformaldehyde vapor to avoid analyte removal by washing, are subsequently embedded in paraffin for sectioning 3–8 μm thick, and are ashed. Each tissue section destined for MEPHISTO analysis is paired with a serial section mounted on a glass slide for histological staining. Tissue and cells may also be embedded in epoxy for ultrathin sectioning, to allow MEPHISTO analysis without ashing.

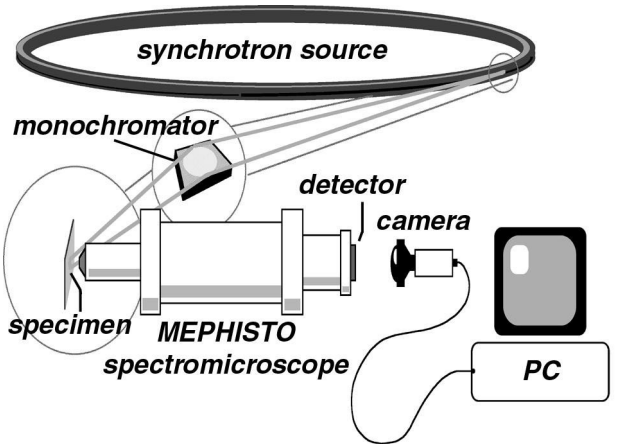

Fig. 1. Experimental set-up for performing spectromicroscopy with MEPHISTO. The essential components are labeled in the diagram and described in the text.The electrostatic lenses which form a magnified, focused electron image of the specimen are located in the body of the spectromicroscope. The synchrotron ring, the monochromator, the sample and the interior of MEPHISTO are all in ultra high vacuum.

3. Results and discussion

3.1. Understanding tissue histology in medical specimens

Local chemical analysis of a biological specimen by spectromicroscopy must be correlated with the histological examination. For the visible light microscope (VLM), this can be deduced from morphological considerations, or by staining of differentiated cells, cell compartments or architecture, or specific proteins. Immunohistochemical stains based on the same principles have been demonstrated for X-ray microscopes and spectromicroscopes [23–25]. The disadvantage of such procedures are that thorough washing steps are required in order to minimize the background stain, which will remove a soluble analyte that is not tightly bound to the tissue. Compared to the VLM, an X-ray spectromicroscope has the additional capability to probe local composition and chemistry. For many experiments, the location of the nucleus is of prime importance, and we have demonstrated that the location of nuclei is revealed by mapping the phosphorus distribution. The DNA bases are connected by phosphodiester linkages, and hence the nucleus as a whole is phosphate rich, as

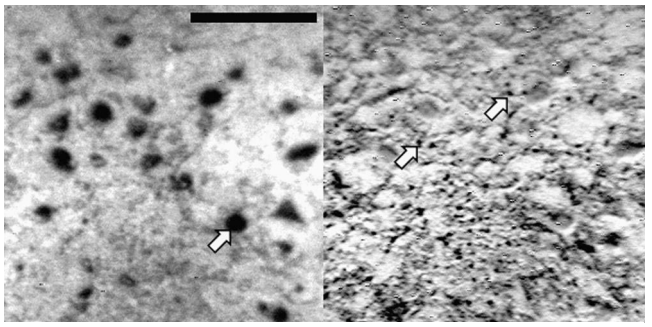

Fig. 2. Phosphate (left) and sulfate (right) maps of ashed human glioblastoma section. In both images, dark areas represent high element concentrations. The phosphate map reveals the distribution of phosphate rich cell nuclei (one is marked by an arrow) as confirmed by histological analysis on serial sections (data not shown). Scale bar = 50 μm. The sulfur map, by comparison, shows no correlation with the nuclei, but smaller sulfur rich spots (arrows) are observed.

shown in Fig. 2 (left). On the right of this figure, the sulfur map of the same tissue area shows, as expected, no correlation with nuclei positions, although much smaller sulfur rich regions are also observed. These are tentatively attributed to areas of protein synthesis, associated with tightly packed intracellular membranes. There are many opportunities to further enable direct cell and cell compartment identification by studying local element and chemical state differences [11,26] and obtaining this information with no extra sample preparation can be a significant improvement. This approach requires the spectromicroscope to be installed on a beamline that can access strong absorption edges of all relevant elements.

3.2. Trace element detection by X-ray absorption spectroscopy

The signal to noise (S/N) ratio of an analyte signal from a microscopic specimen area depends on factors including the local concentration, relative absorption cross section and the probed area. At high concentration, imaging that is based on chemical contrast may be performed at high resolution (<80 nm) for which the performance is limited by the aberrations in the electron optics [27]. At very low analyte concentrations, such chemical imaging is limited by the requirement to obtain a acceptable S/N in an reasonable time [28]. Following a semi-empirical approach [29], the photocurrent of secondary electrons emitted from a specimen surface per unit time can be approximated by $Y = \varphi_o E \mu_l(h\nu) \Delta C_m$, where φ_o is the incident flux density, the photon energy $E = h\nu$, and μ_l is the X-ray linear attenuation coefficient. Δ is an effective depth of the surface layer from which the electrons originate, related to the inelastic mean free path, and C_m is a material constant. The product ΔC_m is fairly independent of energy, and provides a simple link between the theory of photoabsorption and the electron current measured experimentally. With absorption spectra containing statistical noise, the smallest specimen area, A, that allows a spectrum to be acquired with $S/N = k$, where $k = 5$, can then be written, after a few simplifying assumptions [30]:

$$A \geq \frac{k^2}{[\varphi E T \, \Delta C_m \, \rho_C t]} \frac{A_C^2}{N_A^2} \frac{\mu(h\nu)}{\sigma^2(h\nu)} \frac{10^{12}}{[\text{analyte/ppm}]^2}$$

The analyte concentration is expressed here in parts per million, as the ratio of the atomic densities of analyte:matrix, and t is the time taken for the measurement. The detected signal strength varies with the partial photoabsorption cross section, $\sigma(h\nu)$ of the specific analyte core electron (e.g. Gd 3d), and $\mu(h\nu)$ is the total linear attenuation coefficient of the matrix. The factor T includes all contributions to the detection efficiency of the spectromicroscope.

Consider the artificial situation of a uniform trace concentration of gadolinium in an organic matrix: carbon based epoxy. Taking the literature values for carbon (graphite) [31]: its density $\rho_C = 1.7$ gcm^{-1}, atomic mass $A_C = 12$ g, and the mass attenuation coefficient at 800 eV, $\mu = 3 \times 10^3$ cm^2 g^{-1}. At the 3d absorption edge of gadolinium, at 100 ppm concentration, and with empirically determined values for the remaining factors, the smallest specimen area from which a good spectrum can be acquired with $t = 10$ s exposures per point on a second generation synchrotron such as the Synchrotron Radiation Center of the University of Wisconsin-Madison, is a circle of radius 3.2 μm. This value is reasonable, based on experience with spectroscopy in MEPHISTO, although a well-calibrated, trace concentration test specimen against which such estimates could be checked has not been fabricated. For high analyte concentrations, the resolution at which chemical information can be acquired approaches the imaging limits of the electron optics.

In recent work, boron from a BNCT drug was detected in unashed, epoxy-embedded tissue at 80 ppm average concentration, but from acquisition regions of minimum area (50 μm)^2. X-ray absorption spectroscopy of boron in tissue suffers strong interference from phosphorus, which precludes the possibility of ashing to enhance the signal. Nevertheless, the chemical information obtained in the absorption spectra, even at this low concentration, detected evidence of in vivo chemical modification to the BNCT agent [16]. This was an unprecedented result, and relevant to the therapy as its efficacy depends on the fate of the BNCT agent in the tumor.

The situation for a transmission geometry spectromicroscope is simpler, as the attenuation of X-rays follows the Beer–Lambert law, which allows local concentrations to be quantitatively calculated as long as accurate values of the absorption cross section are available [32] and the sample thickness is known (see also [33]). However, transmission spectroscopy has the same high background compared to the total yield mode, but without the signal amplification associated with secondary electron emission,

and hence is likely to be less sensitive. In addition, the probed area cannot be adjusted when a microbeam is employed; instead the sample thickness must be chosen appropriately. Scanning X-ray fluorescence microprobe analysis is by far the most sensitive technique at high energies, because of the substantially lower background, but the radiative yield from the lighter elements ($Z<20$) is very low.

Before performing trace element detection in biological specimens with spectromicroscopy, the bulk averaged analyte concentration is routinely measured by inductively coupled plasma atomic emission spectroscopy (ICP-AES) or mass spectrometry (ICP-MS). In two recent cases of boron and gadolinium based drugs from NCT, administered to human patients, the average concentrations were 80 ppm and 11 ppm respectively. The implication is that in real medical experiments, the detection of trace elements may be close to the detection limit of the technique, even if the samples are ashed to enhance analyte concentration. Thus, the results of spectromicroscopic analysis must be verified against independent techniques, and must be statistically proven, as discussed below.

3.3. Semi-quantitative multicell analyses

Fig. 3 shows a number of cells grown in a culture of human glioblastoma cells, exposed to the potential GdNCT [19] agent Gd-DTPA for 72 h, fixed and ashed, and viewed from the 'top' by the spectromicroscope. The individual cells can be delineated by mapping physiologically present calcium. Each individual cell presents a strong gadolinium spectrum, showing cellular uptake of Gd-DTPA. This result was independently confirmed with Time of Flight Secondary Ion Microscopy analysis of cells from the same specimen. However, this conclusion was only given statistical weight by performing serial analysis on hundreds of cells [17]. Calcium mapping to delineate cells, plus the acquisition of full screen gadolinium X-ray absorption 'movies' (a stack of photoelectron images acquired at photon energies across the Gd M edge from which spatially localized spectra can be extracted) is an efficient method of multicell analysis. These data are an essential demonstration of Gd-DTPA uptake in vitro. Ongoing experiments are studying gadolinium uptake by human brain tumor tissue as the next step in evaluating this gadolinium based therapy.

The lower image of Fig. 3 shows a cell from an equivalent culture, treated in parallel with the cells above, but embedded in epoxy and sectioned 60 rim thick 'vertically' (i.e. normal to the substrate, producing a 'side view') before ashing. High resolution calcium imaging showed small (<1 μm diameter) intracellular compartments, a scale too small for Gd spectroscopy in this case. Subcellular trace element detection without staining remains a challenging goal.

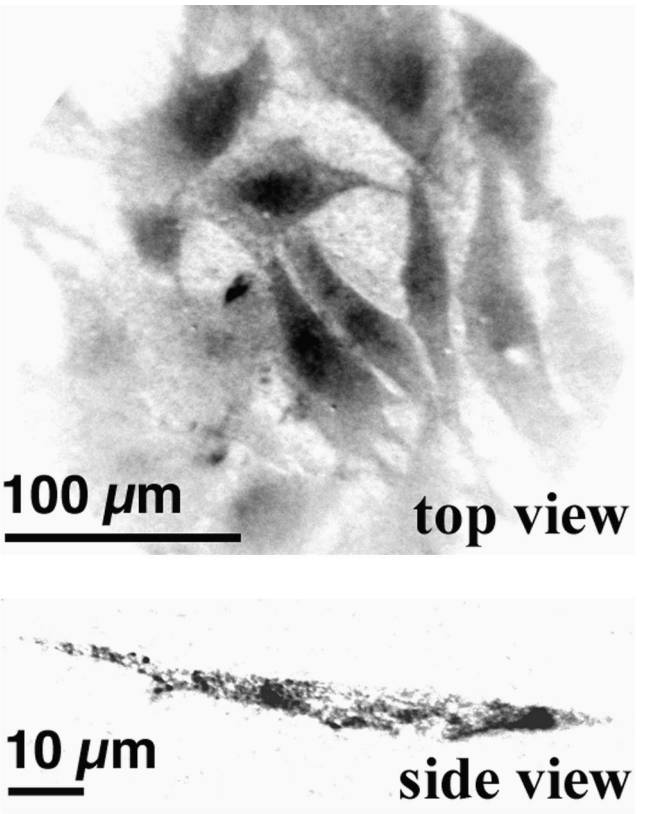

Fig. 3. Maps of the calcium content of cultured glioblastoma cells (Ca is shown dark) that have been analyzed in MEPHISTO to follow the uptake of a gadolinium compound for Gadolinium Neutron Capture Therapy. Images from two equivalent cultures are shown following alternative preparation methods that allow analysis of entire cells ('top view') or vertical thin sections of an individual cell ('side view'). Spectroscopic analysis of many cells revealed a statistically significant tendency for gadolinium to be accumulated at a higher concentration in the nucleus compared to cytoplasmic regions. Top image taken from [22].

4. Conclusions

A number of exciting developments in X-ray imaging include the tomographic reconstruction of three dimensional information [34], and phase contrast imaging to bring out structural details in specimens with poor absorption contrast [35], usually the case with biological specimens. While resolution in the transmission spectromicroscope requires improved Fresnel Zone Plate fabrication technology, abberation corrected electron optics may bring the resolution of electron emission microscopes below 5 nm, while additionally increasing the transmission efficiency [36]. Spectromicroscopes of all kinds have developed methods for the analysis of wet samples [37], as well as sample preparation techniques that limit specimen damage (in the X-ray beam, or prior) and allow analyses to be complementary to conventional optical and electron microscopies. The field of X-ray spectromicroscopy is maturing by both learning from these established microscopies, and by creative improvisation in the areas where it can make a unique contribution.

Acknowledgements

We gratefully acknowledge the generosity and expertise of our collaborators, including M. Neumann and Prof D. Gabel of the University of Bremen for the BNCT tissue samples and Robert Pallini for his collaboration in the GdNCT experiment. We thank Dr. Recep Avci and Dr. David Mogk of Montana State University for invaluable assistance during the ToF-SIMS experiments, and Lingsu Zhang of the University of Wisconsin, Soil Science Department for the ICP-MS analysis. The spectromicroscopy experiments were performed at the Wisconsin Synchrotron Radiation Center, a facility supported by NSF under grant DMR-95-3 1009.

References

[1] K.C. Holmes, Structural biology, Philos. Roy. Soc. B 354 (1999) 1977–1984.
[2] K. Arfelli, V. Bonvicini, A. Bravin, G. Cantatore, E. Castelli, L.D. Palma, M.D. Michiel, M. Fabrizioli, R. Longo, R.H. Menk, A. Olivo, S. Pani, D. Pontoni, P. Poropat, M. Prest, A. Rashevsky, M. Ratti, L. Rigon, G. Tromba, A. Vacchi, E. Vallazza, F. Zanconati, Mammography with synchrotron radiation: phase-detection techniques, Radiology 215 (2000) 286–293.
[3] J.E. Penner-Hahn, Structural characterization of the Mn site in the photosynthetic oxygen-evolving complex, Metal Sites in Proteins and Models 90 (1998) 1–36.
[4] C. Magowan, J.T. Brown, J. Liang, J. Heck, R.L. Coppel, N. Mohandas, W. Meyer-Ilse, Intracellular structures of normal and aberrant Plasmodium-Falciparum malaria parasites imaged by soft-X-ray microscopy, Proc. Natl. Acad. Sci. USA 94 (1997) 6222–6227.
[5] C. Jacobsen, S. Wiliams, E. Anderson, M.T. Browne, C.J. Buckley, D. Kern, J. Kirz, M. Rivers, X. Zhang, Diffraction limited imaging in a scanning transmission X-ray microscope, Opt. Commun. 86 (1991) 351–364.
[6] X. Zhang, H. Ade, C. Jacobsen, J. Kirz, S. Lindaas, S. Williams, S. Wirick, Micro-XANES: chemical contrast in the scanning transmission X-ray microscope, Nucl. Instrum. Meth. A 347 (1994) 431–435.
[7] J. Thieme, G. Schmahl, D. Rudolph, E. Umbach (Eds.), X-ray Microscopy and Spectromicroscopy, Springer, Heidelberg, 1998.
[8] G. De Stasio, M. Capozi, G.F. Lorusso, P.-A. Baudat, T.C. Droubay, P. Perfetti, G. Margaritondo, B.P. Tonner, MEPHISTO: performance tests of a novel synchrotron imaging photoelectron spectromicroscope, Rev. Sci. Instrum. 69 (1998) 2062–2067.
[9] G. De Stasio, L. Perfetti, B. Gilbert, O. Fauchoux, M. Capozi, P. Perfetti, G. Margaritondo, B.P. Tonner, The MEPHISTO spectromicroscope reaches 20 nm lateral resolution, Rev. Sci. Instrum. 70 (1999) 1740–1742.
[10] X. Zhang, R. Balhorn, J. Mazrimas, J. Kirz, Mapping and measuring DNA to protein ratios in mammalian sperm head by XANES imaging, J. Struct. Biol. 116 (1996) 335–344.
[11] C.J. Buckley, N. Khaleque, S.J. Bellamy, M. Robbins, X. Zhang, Mapping the organic and inorganic components of tissue using NEXAFS, J. Physique IV 7 (1997) 83–90.
[12] J. Rothe, E.M. Kneedler, K. Pecher, B.P. Tonner, K.H. Nealson, T. Grundl, W. Meyer-Ilse, T. Warwick, Spectromicroscopy of Mn distributions in micronodules produced by biomineralization, J. Synch. Rad. 6 (1999) 359–361.
[13] P. Blomfield, K. Gough, B. Gilbert, G. de Stasio, Unpublished data.
[14] L.P. Choo, D.L. Wetzel, W.C. Halliday, M. Jackson, S.M. LeVine, H.H. Mantsch, In situ characterization of beta-amyloid in Alzheimer's diseased tissue by synchrotron Fourier transform infrared microspectroscopy, Biophys J. 71 (1996) 1672–1679.
[15] H. Benveniste, G. Einstein, K.R. Kim, C. Hulette, G.A. Johnson, Detection of neuritic plaques in Alzheimer's disease by magnetic resonance microscopy, Proc. Natl. Acad. Sci. USA 96 (1999) 14079–14084.
[16] B. Gilbert, L. Perfetti, O. Fauchoux, J. Redondo, P.-A. Baudat, R. Andres, M. Neumann, S. Steen, D. Gabel, D. Mercanti, M.T. Ciotti, P. Perfetti, G. Margaritondo, G. De Stasio, The spectromicroscopy of boron in human glioblastomas following administration of BSH, Phys. Rev. E, in press.
[17] G. De Stasio, P. Casalbore, B. Gilbert, D. Mercanti, M.T. Ciotti, L.M. Larocca, A. Rinelli, D. Perret, D.W. Mogk, P. Perfetti, R. Pallini, Gadolinium in human glioblastoma cells for gadolinium neutron capture therapy (Gd-NCT), submitted to Cancer Res.
[18] R.F. Barth, A.H. Soloway, J.H. Goodman, R.A. Gahbauer, N. Gupta, T.E. Blue, W.L. Yang, W. Tjarks, Boron neutron capture therapy of brain tumors: An emerging therapeutic modality, Neurosurgery 44 (1999) 433–450.
[19] J.A. Shih, R.M. Brugger, Gadolinium as a neutron capture therapy agent, in: B.J. Allen, D.E. Moore, B.V. Harrington (Eds.), Progress in Neutron Capture Therapy, Plenum Press, New York, 1992, pp. 183–186.
[20] G. De Stasio, D. Dunham, B.P. Tonner, D. Mercanti, M.T. Ciotti, A. Angelini, C. Coluzza, P. Perfetti, G. Margaritondo, Neuroreport 4 (1993) 1175–1178.
[21] G. De Stasio, B. Gilbert, L. Perfetti, R. Hansen, D. Mercanti, M.T. Ciotti, R. Andres, V.E. White, P. Perfetti, G. Margaritondo, Cell ashing for trace element analysis: a new approach based on UV/Ozone, Anal Biochem. 266 (2) (1999) 174–180.
[22] B. Gilbert, L. Perfetti, R. Hansen, D. Mercanti, M.T. Ciotti, P. Casalbore, R. Andres, P. Perfetti, G. Margaritondo, G. De Stasio, UV/Ozone ashing for spatially resolved trace element analysis, Frontiers in Bioscience 5 (2000) 10–17, http://www.bioscience.org/2000/v5/algilbert/fulltext.htm.
[23] H.N. Chapman, C. Jacobsen, S. Williams, A characterisation of dark-field imaging of colloidal gold labels in a scanning transmission X-ray microscope, Ultramicroscopy 62 (1996) 191–213.
[24] B. Gilbert, M. Neumann, S. Steen, D. Gabel, R. Andres, P. Perfetti, G. Margaritondo, G. De Stasio, Immunohistochemistry for the MEPHISTO X-PEEM, Proceedings of X-Ray Microscopy and Microanalysis XRM99, Berkeley, CA, August 2–6, 1999, in press.
[25] M.M. Moronne, Ultramicroscopy 77 (1999) 23–36.
[26] J. Boese, A. Osanna, C. Jacobsen, J. Kirz, Carbon edge XANES spectroscopy of amino acids and peptides, J. Elec. Spectrosc. Rel. Phenom. 85 (1997) 9–15.
[27] E. Bauer, The possibilities for analytical methods in photoemission and low-energy microscopy, Ultramicroscopy 36 (1991) 52–62.
[28] G. Margaritondo, The information content of photoemission spectroscopy and spectromicroscopy, Surface Rev. Let. 2 (1995) 305–313.
[29] J. Stohr, Nexafs Spectroscopy, Springer, Berlin, 1992.
[30] B. Gilbert, PhD Thesis (2000).
[31] J.H. Hubbell, S.M. Seltzer, Tables of X-ray mass attenuation coefficients and mass energy-absorption coefficients (Version 1.02), [Online] in: 1997, Available at: http://physics.nist.gov/xaamdi.
[32] C.J. Buckley, The measuring and mapping of calcium in mineralized tissues by absoption difference mapping, Rev Sci. Instrum. 66 (1994) 1318–1321.
[33] S. Rondot, J. Cazaux, Experimental verification of a new quantification procedure for elemental mapping by analytical X-ray microscopy, Ultramicroscopy 65 (1996) 159–177.
[34] Y. Wang, C. Jacobsen, J. Maser, A. Osanna, Soft X-ray microscopy with a cryo scanning transmission X-ray microscope: II. Tomography, J. Microscopy 197 (2000) 80–93.

[35] Y. Hwu, B. Lai, D.C. Mancini, J.H. Je, D.Y. Noh, M. Bertolo, G. Tromba, G. Margaritondo, Coherence based contrast enhancement in X-ray radiography with a photoelectron microscope, Appl. Phys. Lett. 75 (1999) 2377–2379.
[36] G.F. Rempfer, M.S. Mauck, Correction of chromatic aberration with an electron mirror, Optik 92 (1992) 3–8.
[37] G. De Stasio, B. Gilbert, T. Nelson, R. Hansen, J. Wallace, D. Mercanti, M. Capozi, P.A. Baudat, P. Perfetti, G. Margaritondo, B.P. Tonner, Transmission spectromicroscopy in the water window: a feasibility test with the MEPHISTO system, Rev. Sci. Instrum. 71 (2000) 11–14.